JOURNAL OF CRITICAL REVIEWS

ISSN- 2394-5125 VOL 5, ISSUE 07, 2018

ELECTRO-HYDRAULIC ACTIVE SUSPENSION MODELING AND CONTROL

SK HUSSIAN BASHA 1, PRAVEEN KUMAR MUNNANGI 2,
ASSISTANT PROFESSOR 1,2
Mail ID; hussainn.shaik@gmail.com, Mail ID:praveenmunnangi009@gmail.com
Dept.: Mechanical
Nagole Institute of Technology and Science,
Kuntloor(V),Hayathnagar(M),Hyderabad,R.R.Dist.-501505.

Abstract

There is less of a compromise needed between ride quality and handling with an active suspension system. In order to do this, appropriate actuators will need to be used, which will need precise regulation. In this article, a model-based controller for a nonlinear suspension actuator is proposed. First, the idea is developed in the linear framework to make the latter stages of synthesis and analysis more manageable. A linear actuator model is presented and explained in that section. In addition, a two-degree-of-freedom controller that may independently mildly reference and disturbance responses is developed and contrasted with model-free PID controllers during this design phase. Next, a linear parameter variable representation of the nonlinear plant is taken into account, and the better two-degree-of-freedom controller is fitted to the nonlinear framework. At last, a test vehicle is used to prove that the nonlinear controller can be used in practice.

Introduction

Passenger automobiles' ride and handling are greatly impacted by the suspension system. Passive suspension systems usually need a compromise between competing criteria describing road handling and passenger comfort throughout the design process. But active suspensions made feasible by sensors, controllers, actuators, and a data processing unit may apply more suspension forces on demand, easing the tension between ride quality, handling, and safety. Such suspensions often have a two-tiered control scheme. Different control techniques, from the simple skyhook controller to the intricate optimum controller design methods [1, 2], have been examined in order to identify how the vehicle body controller calculates the additional forces required for the real driving state. On a more fundamental level, the actuator controller must ensure that the actuator produces the specified reference force as specified by the vehicle body controller. Most studies on active suspension systems (e.g. [3]– [6]) treat the actuator as a perfect source of force, ignoring the fact that it has its own internal dynamics that interact in various ways with the vehicle's overall dynamics. Actually, most actuators have nonlinear behaviour [7], have a restricted bandwidth [8], and are subject to ex ternal disturbances, which increases the complexity of the controller design and places extra demands on the controller design procedure. Moreover, realizing active suspensions has often been the subject of purely theoretical studies with little relevance to actual application.

Modelling and describing the system

The actuator shown in Fig. 1a consists of a standard shock absorber cylinder, two movable valves to provide unidirectional damping resistance, and two accumulators to compensate for volume change in the cylinder chambers. The actuator mimics the behaviour of a passive spring-damper in this setup. A power-pack consisting of a hydraulic pump and an electric motor is added so that active forces may be exerted, i.e., regardless of the amplitude and sign of deflection velocities Ze.

A mathematical model that is nonlinear

When the system needs it, accumulators may release their stored hydraulic energy. Assuming the gas undergoes a polytropic phase transition, the

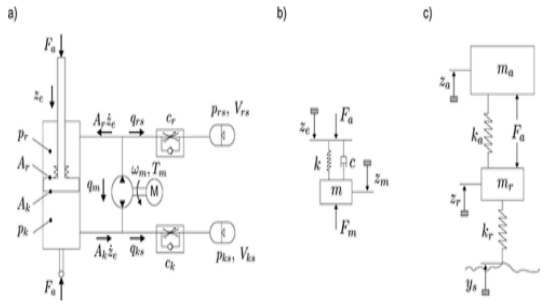

Figure 1: A quarter-car model with a nonlinear actuator (a) and a linearized actuator (b) based on [9]. (c)

FIGURE 1A: Pressure in the bottom accumulator, for which the following state equation may be derived

$$p_{ks}V_{ks}^{\kappa} = p_0 V_{k0}^{\kappa} \quad \text{or} \quad p_{ks} = p_0\left(\frac{V_{k0}}{V_{ks}}\right)^{\kappa}$$

:

where p0 is the static charge pressure, Vk0 is the starting gas volume, Vks = Vk0 − R qksdt is the actual gas volume owing to fluid flow qks, and κ is the poly tropic gas constant. Differentiating (1)

ISSN- 2394-5125 VOL 5, ISSUE 07, 2018

with regard to time and inserting V˙ KS = −qks provides the state equation of the pressure rate of change

Analogously, the state equation for

$$\dot{p}_{ks} = p_0 \kappa \left(\frac{V_{k0}}{V_{ks}}\right)^{\kappa-1} \left(-\frac{V_{k0}}{V_{ks}^2}\dot{V}_{ks}\right) = \kappa p_0 \left(\frac{V_{k0}}{V_{ks}}\right)^{\kappa} \left(\frac{-\dot{V}_{ks}}{V_{ks}}\right) = \kappa\, q_{ks}\frac{p_{ks}}{V_{ks}}.$$

The equation of motion of the pump reads as

$$\dot{p}_{rs} = \kappa q_{rs}\frac{p_{rs}}{V_{rs}}.$$

the upper gas accumulator in Fig. 1a is

$$J_m\dot{\omega}_m = T_m - \frac{V_c}{2\pi}(p_k - p_r)$$

where m is the rotary speed of the pump, JM is the angular momentum of the combined mass of the motor and pump, Vc is the capacity coefficient of the pump, pk and pr are the pressures in the cylinders, and Tm is the torque applied to the motor. Pump flow is calculated as follows:

$$q_m = \frac{V_c}{2\pi}\,\omega_m.$$

The actuator force is calculated from both pressures acting on the piston:

$$F_a = p_k A_k - p_r A_r = (p_{ks} + \Delta p_{ks})A_k - (p_{rs} + \Delta p_{rs})A_r$$

where Ak and AR are the surfaces of the piston in the two respective cylinder chambers. The pressure drops Δpks and Δprs result from the damping valves as

$$\Delta p_{ks} = p_k - p_{ks} = q_{ks}c_k, \quad \Delta p_{rs} = p_r - p_{rs} = q$$

Where

$$c_k = c_k(q_{ks}), \quad c_r = c_r(q_{rs})$$

are the nonlinear characteristics of the valves depending on the flows through the valves? The characteristics correspond to those of valves used in conventtional shock absorbers. With the suspension deflection Ze, the internal fluid flows in the actuator are balanced to

$$q_{ks} = q_m + \dot{z}_e A_k, \quad q_{rs} = -q_m - \dot{z}_e A_r.$$

Substituting qks from (9) and qm from (5) in (2) yields

$$\dot{p}_{ks} = \kappa\ (q_m + \dot{z}_e A_k)\frac{p_{ks}}{V_{ks}} = \kappa\ \left(\frac{V_c}{2\pi}\ \omega_m + \dot{z}_e A_k\right)\frac{p_{ks}}{V_{ks}}.$$

Techniques for Maintaining Order

However, high frequency performance may suffer if significant damping forces are used to suppress the resonance peak of the sprung mass representing the car's body. The ideal skyhook control is often proposed as a body controller in an attempt to resolve this inconsistency. In this suspension setup, the damper is effectively located between the sprung mass and the inertial reference frame, which in this case is the sky. For this strategy to be used in practice, the car's active suspension would have to deliver forces that are proportionate to the velocity of the sprung mass

$$F_{a,ref} = -\dot{z}_a C_{SH}$$

where CSH is the dampening of the skyhook. The actuator controller will use the value Fare as its input reference force. Cancellation of the sprung mass resonance peak is the goal of the skyhook control system, whereas at higher frequencies the skyhook should be ineffectual and behave like a passive damper. However, this objective can only be achieved if the actuator controller functions as intended and can handle frequent and intense fluctuations. The following describes the development and analysis of two distinct types of actuator controllers for use with the modified quarter-car model: first, two proportional-integral-derivative (PID) controllers, and second, a 2-degrees-of-freedom (2-DOF) controller with a feed-forward and feedback route.

Analog proportional integral derivative (PID) controllers

Feedback control using proportional, integral, and derivate (PID) is shown in Fig. 2a. Input to the PID controller is an error signal calculated by comparing the reference force Fare with the measured output signal Fa. In Fig. 1b, the actuator receives an input force Fm that is proportional to

ISSN- 2394-5125 VOL 5, ISSUE 07, 2018

three signals: the error signal, its derivative, and its integral. These three signals are combined to provide the output of the PID controller.

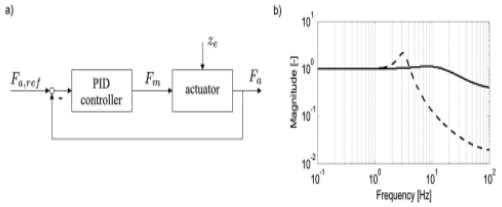

Figure 2: (a) high bandwidth (solid) and (b) low bandwidth (dashed) controller frequency responses, representing the PID control technique.

Two distinct PID controllers were developed for this application using loop-shaping, or modifying the closed-loop system's frequency response [10]. Because of its large closed-loop bandwidth, the first controller (PID-H) ensures reliable tracking performance. In order to strike a balance between excellent tracking and a bandwidth smaller than the un-sprung mass mode, the second controller (PID-L) is built. In Fig. 2b, the transfer function is described in terms of the frequency responses of both closed-loop systems.

$$G_{cl} = \frac{F_a}{F_{a,ref}}.$$

When comparing systems with different bandwidths, we see that the one with the lower bandwidth has a smaller ResoNance peak, indicating that it has a weaker tracking performance even at low frequencies. The actuator's internal dynamics generate the peak.

Controller with just two degrees of freedom

A second kind of control relies on the plant's own internal model.

$$F_a(s) = (cs + k)(z_e - z_m),$$ resulting in

$$z_m = z_e - \frac{F_a}{cs + k}.$$

When the velocity vm = szm is added, the perfect feed forward control rule is achieved, since the speed of the electric pump motor is more amenable to regulation than its location.

$$v_m = -\frac{s}{cs + k}F_a + sz_e.$$

In practice, the reference actuator force Fa, ref required by the body controller is used in place of the actual actuator force Fa. It is necessary to use a disturbance controller to manage the rejection of disturbances.

$$K_{dd} = sG_{tp}$$

consisting of a derivation defined by (31), and a low pass filter whose transfer function is The Ze deflection signal is measured, and then Gtp is applied to it (t). Because of this, the actuator's reference velocity may be controlled by a feed-forward law.

$$v_{m,ref} = -\frac{s}{cs + k}F_{a,ref} + K_{dd}z_e.$$

An internal PID feedback control loop ensures that the reference actuator velocity is maintained, and a PI controller with transfer function Kss weakly follows the reference force (see Fig. 3). Because of the two-degree-of-freedom control architecture, we can independently mold the reference and disturbance responses. The low-gain feedback control law Kss (dotted path) is employed to reduce the steady-state error in the force, while the rapid dynamics necessary for reference tracking (solid black route) is decoupled from this law. Additionally, the low-pass filter Gtp is used independently of Kidd to control the disturbance rejection (Gray path). The effectiveness of the active suspension system depends heavily on selecting the appropriate sequence and cut-off frequency for the disturbance filter. Since the high frequency content of the suspension force Fa will not perturb the controller via feedback of vm in contrast to the force feedback control in Fig. 2a, a velocity control loop with a large bandwidth is now possible. However, the velocity control loop may be strong enough to counteract the m-inertia actuator's effects and account for the possibility of friction in the motor-pump.

ISSN- 2394-5125 VOL 5, ISSUE 07, 2018

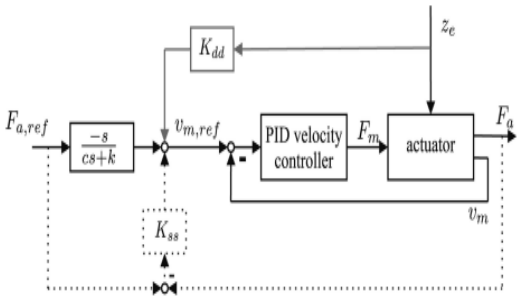

Flowchart of the proposed linear 2-DOF control method

The need to make the actuator work as a passive system for high-frequency deflections drives the implementation of low-pass filter Gtp in (32). Therefore, the disturbance filter should be made in a way that causes it to reject low-frequency disturbances while passing on high-frequency information. The dynamics of the closed-loop actuator are shown in Fig. 3 and must be solved for the filter Gtp.

$$F_a(s) = T(s)F_{a,ref}(s) + S(s)z_e(s)$$

Schematic depicting the suggested linear 2-degree-of-freedom control mechanism

Implementing low-pass filter Gtp in order to make the actuator function as a passive system for high-frequency deflections (32). That's why it's important to design the disturbance filter such that it can block out noise at higher frequencies while letting through noise at lower ones. For the filter Gtp, the dynamics of the closed-loop actuator are depicted in Fig. 3.

$$G_a(s) = \frac{s^2 z_a}{y_s}.$$

Furthermore, we use the dynamic tire load as an indicator for the road contact to evaluate the ride safety. It can be expressed in the frequency domain as:

$$G_{tl}(s) = k_r \frac{z_r - y_s}{y_s}.$$

Figure 4 is a visual representation of the four possible suspension setups, including the passive suspension (Gray, zm = 0) and three active suspension setups. The PID controllers described in Section 3.1 are used to regulate two of the active suspensions; these are the high gain variation PID-H (dotted) and the low gain variant PID-L. (dashed). The 2-degrees-of-freedom controller (solid black) from the previous section provides the force control for the third active suspension.

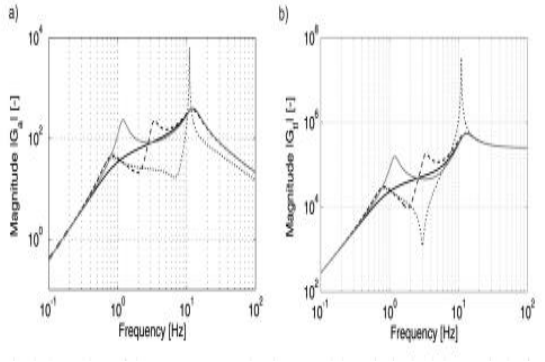

Figure 4: Passive (Gray), 2-DOF (solid black), PID-H (dotted), and PID-L (solid) regulate sprung mass acceleration (a) and dynamic tire load (b) magnitudes (dashed)

See Fig. 4a for a visual representation of the linear frequency responses demonstrating that all three controllers achieve comparable results in dampening the bounce acceleration towards the sprung mass mode (0.5 2Hz). But the PID-H controller's un-sprung mass mode exhibits an unfavourable resonance peak. The high controller bandwidth, which optimally implements the skyhook damping notion, has this impact. Even though the damping coefficient is greater than the passive system's integral damper, it is only used to damp the sprung mass's minute vibrations. The passive damper is connected to the considerably larger deflections of the suspension. In line with what was expected during design, we find that the PID-L controller with a bandwidth less than the un-sprung mass mode has superior high frequency features. Resonance peak shown in Fig. 2b clearly degrades performance at about 3Hz for mid-range frequencies. Resonance peaks at 14Hz and 3Hz for the PID-H and PID-L controllers may be seen in the dynamic tire load curve in Fig. 4b. Both the sprung mass acceleration and the dynamic ic tire load benefit from the more uniform frequency response achieved by the suggested 2-DOF approach. It is self-evident that this accomplishes the control goals of attenuating low frequencies and providing a response analogous to the passive system at higher frequencies.

A Non-Linear Actuator Since the linearized model is only correct close to the operating point, it cannot characterize the nonlinear actuator's

ISSN- 2394-5125 VOL 5, ISSUE 07, 2018

behavior over the whole working range. However, the nonlinear actuator model may also benefit from the given 2-DOF control strategy by using the linear parameter-varying (LPV) system theory [11]. The LPV model, in contrast to linearization techniques, enables us to take into account nonlinear effects in the representation of the state space. The mathematical expression for a linear system with time-varying parameters is

$$\dot{\boldsymbol{x}} = \boldsymbol{A}(\boldsymbol{\rho}(t))\,\boldsymbol{x} + \boldsymbol{B}(\boldsymbol{\rho}(t))\,\boldsymbol{u},$$
$$\boldsymbol{y} = \boldsymbol{C}(\boldsymbol{\rho}(t))\,\boldsymbol{x} + \boldsymbol{D}(\boldsymbol{\rho}(t))\,\boldsymbol{u}$$

where (t) is an online-measurable limited time-varying parameter vector. The nonlinear state equations (16) in this situation may be re-interpreted as an LPV system with time-varying parameters.

$$\rho(t) = \left[\frac{p_{ks}}{V_{ks}} \quad \frac{p_{rs}}{V_{rs}} \quad c_k \quad c_r\right]^T = \left[\frac{p_{ks}^{1+1/\kappa}}{V_{k0}p_0^{1/\kappa}} \quad \frac{p_{rs}^{1+1/\kappa}}{V_{r0}p_0^{1/\kappa}} \quad \bar{c}_k(q_m, \dot{z}_e) \quad \bar{c}_r(q_m, \dot{z}_e)\right]$$

where we assume that the states pks(t), prs(t), the input ˙Ze(t) and the pump flow qm(t) are measurable. The second notation in equation (44) is obtained from equations (1), and (9) by substituting

$$\dot{V}_{ks} = V_{k0}(p_0/p_{ks})^{1/\kappa},$$

$V_{rs} = V_{r0}(p_0/p_{rs})^{1/\kappa}$ and $c_k(q_{ks}) = c_k(q_m + \dot{z}_e A_k) =: \bar{c}_k(q_m, \dot{z}_e)$, $c_r(q_{rs}) = c_r(-q_m - \dot{z}_e A_r) =: \bar{c}_r(q_m, \dot{z}_e)$. Since m, ref in Fig. 5 is equivalent to vm, ref in Fig. 3, we may modify the control section of Fig. 3 to work with the LPV system (43). The inverted plant model, like the linear notion, results in a control system that incorporates feed-forward control (the solid black route) and a disturbance rejection component (Gray path). In addition, the dotted route represents the addition of a low-gain feedback control. Furthermore, we see that the control rule accounts for the asymmetrical nature of the system by making a distinction between the Ak and AR sectors of the pistons.

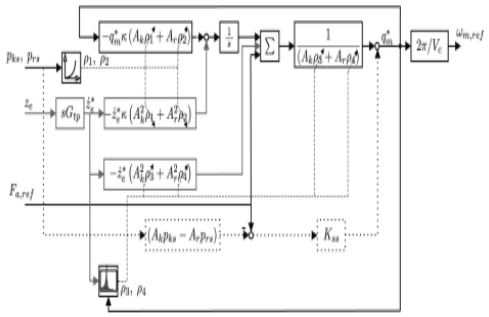

The suggested nonlinear 2-degrees-of-freedom (DOF) control method is shown in Fig. 5.

The nonlinear actuator's control method was put through its paces on an experimental setup. To do this, a second servo-hydraulic actuator was employed to excite the actuator shown in Fig. 1a, with a typical suspension deflection signal serving as the displacement command signal. In addition, the controller took in information in the form of a reference force signal. There were two actualized experiments. The controlled actuator was used in the second experiment, whereas the passive system (m = 0) was activated in the first. A satisfactory reference tracking performance is attained for low frequent force components when the control system is active, as shown by the observations in Fig. 6b. As can be seen in Fig. 6a and anticipated by the frequency response in Fig. 4, the high-frequency differences responsible for dampening the un-sprung mass mode are almost equal to those of a passive damper. The control goals established during the design phase are verified to have been met by the actual nonlinear system as a consequence of the experiments.

Comprehensive command of the automobile

A test vehicle was built using the 2-degrees-of-freedom control strategy described in the preceding section. As a result, changes had to be made to the statute regulating automobile bodies.

ISSN- 2394-5125 VOL 5, ISSUE 07, 2018

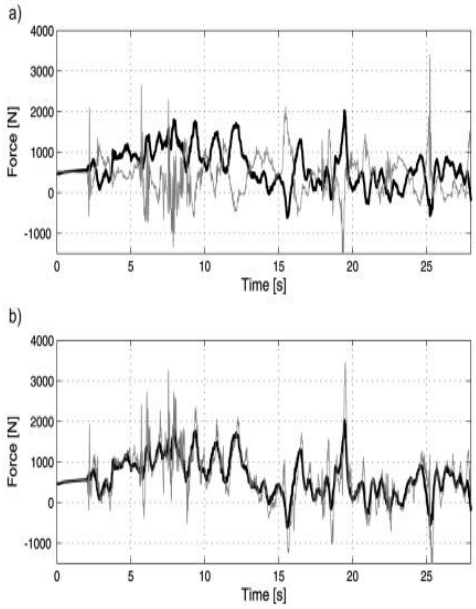

Fig. 6 Contrast of the passive (a) and controlled (b) actuator's reference force test signal (black) and measured force signal (Gray).

(27) to the chassis of the whole vehicle. A full-car body controller concept is seen in Fig. 7 and is based on a linear, vertical full-car model. A spatially sprung mass is linked to four unsprang masses, one at each corner of the model. The vehicle's body is driven by use of a modal control method. The heave zH, roll R, and pitch P modal movements must be evaluated and managed in this setup. Virtual forces and moments on the skyhook are determined, in particular, by evaluating the first derivatives of the modal states.

$$\boldsymbol{F}_V = \begin{bmatrix} F_H \\ M_R \\ M_P \end{bmatrix} = \begin{bmatrix} -\dot{z}_H C_{SH,H} \\ -\dot{\varphi}_R C_{SH,R} \\ -\dot{\varphi}_P C_{SH,P} \end{bmatrix}$$

in where the heave, roll, and pitch damping parameters CSH, H, CSH, R, and CSH, P are the skyhook damping constants. Then, the virtual modal amounts are assigned as reference forces to the four operational actuators.

$$\boldsymbol{F}_{a,ref} = \begin{bmatrix} F_{a,ref,fl} & F_{a,ref,fr} & F_{a,ref,rl} & F_{a,ref,rr} \end{bmatrix} = \boldsymbol{M}\boldsymbol{F}_V$$

$$\boldsymbol{M} = \frac{1}{(l_f + l_r)(w_f + w_r)} \begin{bmatrix} l_r w_r & l_r & -w_r \\ l_r w_l & -l_r & -w_l \\ l_f w_r & l_f & w_r \\ l_f w_l & -l_f & -w_l \end{bmatrix}$$

The matrix represents a constant distribution. The actuator controllers, which are carbon copies of the nonlinear con troller in Fig. 5, take their input from the reference force signals (48). Accumulator pressure and suspension deflection at each corner are given back to the controllers to be used in generating the electric motors' reference angular velocity signals.

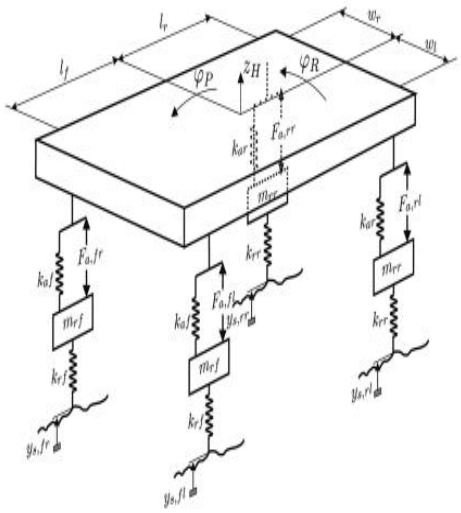

Model of a whole automobile shown in a linear trajectory

This software and hardware were installed in a test vehicle, which was then driven at 70 kilometres per hour across a special track. Different setups were tried out in following experiments. In the first setup, the passive suspension is paired with a softer valve setting, while in the second, the damping valves are in the harsh mode. The third setup, which employs the active mode with the nonlinear actuator controller, is the most intriguing of the three. The modal acceleration signals zH, R, and P are subjected to a power spectral density (PSD) analysis with normalization for the purpose of nonlinear model assessment. Figure 8 shows that the hard setting (dashed) of the passive system significantly dampens the accelerations of the bounces around the sprung mass mode. However, when we increase the frequency, we see a decline in performance, particularly in the intermediate frequencies (2-8Hz), where noise is most noticeable. Exactly as was predicted, the active

ISSN- 2394-5125 VOL 5, ISSUE 07, 2018

system (solid black) outperforms the soft passive system (Gray) at low frequencies while being on par with it at high frequencies. Nonlinear PSD analysis confirms frequency zones with considerable vibration reduction, which is consistent with the frequency response of the linear systems shown in Fig. 4.

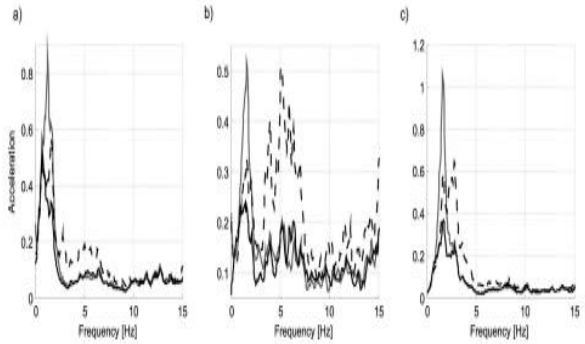

Figure 8 shows a PSD analysis of the heave (a), roll (b), and pitch (c) modal accelerations of the test vehicle's body for three different suspension setups: passive with soft damping (Gray), passive with strong damping (dashed), and active with the nonlinear 2-degrees-of-freedom controller. (Dark as night)

Conclusions

A linearized and simplified model of the control plant served as the basis for the control strategy given in this study. This enables us to compare the performance of two distinct controller ideas in the frequency domain, with the 2-DOF controller emerging victorious over two distinct PID controllers. A nonlinear 2-degree-of-freedom (DOF) controller is designed and validated on an experimental test rig using this finding and an LPV representation of the nonlinear model. The results of the experiments demonstrate a good disturbance response with decent force tracking capability. In addition, tests performed on a genuine test vehicle validate the active suspension system's ability to significantly enhance the ride performance of the vehicle. Compared to a soft passive damper, the number of vibrations at higher frequencies is maintained while the low-frequency vibrations are significantly reduced by the two-degree-of-freedom control. As part of their current work, the authors are developing a preview technique to enhance the efficiency of the provided control idea [12] and putting it to the test in a real vehicle.

REFERENCES

[1] Cao J., Liu H., Li P., Brown D.J.: State of the Art in Vehicle Active Suspension Adapttie Control Systems Based on Intelligent Methodologies. IEEE Transactions on Intelligent Transportation Systems, Vol. 9, pp. 392-405, 2008.

[2] Cao D., Song S., Ahmadian M.: Editors' Perspectives: Road Vehicle Suspension Design, Dynamics, and Control. Vehicle System Dynamics, Vol. 49, pp. 3-28, 2011.

[3] Esmail Zadeh E., Taghirad H.D.: State-Feedback Control for Passenger Ride Dynamics. The Transactions of the Canadian Society for Mechanical Engineering, Vol. 19, pp. 495-508, 1995.

[4] Filho I., Balas G.J.: Road Adaptive Active Suspension Design Using Linear ParameterVarying Gain-Scheduling. IEEE Transactions on Control Systems Technology, Vol. 10, pp. 43-54, 2002.

[5] Du H., Zhang N.: Constrained H∞ Control of Active Suspension for a Half-car Model with a Time Delay in Control. Proceedings of IMechE, Part D: Journal of Automobile Engineering, Vol. 222, pp. 665-508, 2008.

[6] Bultmann B., Herrera E., Hulse A., Figured J., Junking L., Markee M., Ambrose R.O.: An Active Suspension System For Lunar Crew Mobility. IEEE Aerospace Conference, Big Sky, MT, USA, pp. 1-9, 2010.

[7] Lauwerys C., Swevers J., Sas P.: Linear Control of Car Suspension Using Nonlinear Actuator Control. Proceedings of the International Conference on Noise and Vibration Engineering, Leuven, Belgium, pp. 55-61, 2002.

[8] Koch G., Fritsch O., Lohmann B.: Potential of Low Bandwidth Active Suspension Control with Continuously Variable Damper. Proceedings of the 17th IFAC World Congress, Seoul, Korea, pp. 3392-3397, 2008.

[9] Cytrynski S.: Federungssystem fur ein Fahrzeug. Patent DE102010007237A1, 2010. ¨ [10] Cominos P., Munro N.: PID Controllers: Recent Tuning Methods and Design to Specification. IEE Proceedings – Control Theory and Applications, Vol. 149, pp. 46-53, 2002.

[11] Kamen E.W., Khargonekar P.P.: On the Control of Linear Systems whose Coefficients Are Functions of Parameters. IEEE Transactions on Automatic Control, Vol. 29, pp. 25-23, 1984.

[12] Ajala O., Bustle D., Rauh J., Ammon D.: Zero-phase Filtering Control of an Active Suspension System with Preview. Proceedings of

ISSN- 2394-5125 VOL 5, ISSUE 07, 2018

the 11th International Symposium on Advanced Vehicle Control, Seoul, Korea, 2012